Nov 8th, 12:00 AM

Strength of Composite Cold-formed Steel-concrete Beams

Richard P. Nguyen

Ninth International Specialty Conference on Cold-Formed Steel Structures
St. Louis, Missouri, U.S.A., November 8-9, 1988

STRENGTH OF COMPOSITE COLD-FORMED STEEL-CONCRETE BEAMS

By Richard P. Nguyen,[1] Member, ASCE

INTRODUCTION

In recent years, thin-walled, cold-formed steel structural members have gained increasing use in building construction and different types of structural systems [3,10,11]. The use of these members in composite steel-concrete beams has been very limited even thougth the composite cold-formed steel-concrete slabs have been used extensively in building construction and other areas [4,5,7]. The construction of cast-in-place concrete beams requires the installation and removal of form work and shoring, which constitutes a considerable part of their costs. However, the above mentioned construction cost can be significantly reduced if the conventional steel reinforcing bar is replaced by a thin-walled cold-formed steel channel section as forms to carry the wet concrete during construction stage and to function as reinforcement in composite reinforced concrete beams. Test results show that by replacing standard reinforcement with thin-walled cold-formed steel section of equal cross sectional area, the structural strength of the beam is maintained while saving is achieved in the cost of forms and shoring. This paper

---

[1]Associate Professor of Civil Engineering, California State Univ. at Long Beach, Long Beach, CA 90840.

discusses the test program used in the experimental study and the development of the empirical formula to be used for evaluating the ultimate shear bond capacity of composite cold-formed steel-concrete beam members and the behavior of these members under bending and combined bending and shear.

EXPERIMENTAL INVESTIGATION

The objectives of the experimental investigation have been to determine the bending and shear capacities of composite cold-formed steel-concrete beams and to study the behavior of these beams under a combination of shear and bending stresses. Design formulas were also developed to predict the shear strength and the bending capacities of these beam members.

A total of 32 full size beam specimens were tested in this program. The first 16 beam specimens were tested under shear, four of them under bending and the remaining 12 beams were tested subjected to a combination of shear and bending. These composite reinforced concrete beam specimens were fabricated by using cold-formed steel channel as principal reinforcement.

COLD-FORMED STEEL SOFFIT SECTIONS

The function of cold-formed steel soffits in composite beams is similar to that of cold-formed steel panels in composite floor decking systems [4,7]. In both cases, the thin-walled cold-formed

steel performs a dual role as form during construction phase and as positive reinforcement after concrete hardens. Subsequently, concrete and cold-formed steel soffit will act as a composite reinforced concrete beam. The channels were fabricated from gavanized cold-formed steel sheet with round embossments in their web area to improve the bonding characteristic between concrete and steel. The diameter of the embossments is 0.5 inch and and their depth is 0.25 inch. The distance between embossment is 4 inch on center in the web area along the length of the channel. Fig. 1 shows the dimensions and location of the embossments in the channel. The thickness of the channel varies from 0.0499 inch to 0.0806 inch and the channel's depth ranges from 3.872 inches to 6.125 inches. Fig. 2 is a photo of a typical cold-formed steel channel used in this testing program. Table 1 lists the dimensions of the cold-formed steel channel sections for all 32 beam test specimens

COMPOSITE BEAMS

The composite beams used in this experimental study are made of concrete and thin-walled cold-formed steel stiffened channel sections. Fig. 3 depicts a typical section of these beam specimens and Table 2 lists the actual cross-sectional dimensions and span lengths for all beam specimens used in this experimental investigation. For each beam specimen, the ultimate compressive strength of concrete, the yield point of cold-formed steel channel, the cross sectional area of steel, the steel ratio in the

beam section are also tabulated in Tables 1 and 2. The function of cold-formed steel is to support the fresh concrete prior to the concrete curing and strength gain. Once the concrete has been placed, cured, and gained sufficient strength, the beam is designed as a composite reinforced concrete members in which the cold-formed steel channel performs as reinforcement for the composite beams. Following is a summary of the pertinent parameters of beam specimens used in the testing program:

1. Ultimate compressive strength of concrete
2. Yield strength of cold-formed steel channel
3. Thickness of cold-formed steel channel
4. Width of cold-formed steel channel
5. Cross sectional area of cold-formed steel channel
6. Depth of the composite beam
7. Span length of beam specimen
8. Shear length of beam specimen
9. Reinforcement ratio of composite cold-formed steel composite beam
10. Cold-formed steel channel type and embossment

TEST PROGRAM

In this experimental investigation, three series of tests were conducted on composite beams using cold-formed steel stiffened channels as their soffits. Series A which consists of 15 beam specimens, examined the shear strength of the composite beams by

using test setup Type I and Type II as shown in Figures 4 and 5. Series B tested four beam specimens under pure bending by using test setup Type II (Fig. 5) to verify the flexural capacities of the composite cold-formed steel-concrete beams. Series C examined the behavior of 12 beam specimens under a combined bending and shear stresses by using test setup Type I as indicated in Fig. 4.

Each beam specimen was tested under a simply supported condition. Rollers and bearing plates were provided at each end and at the locations of applied loads. For Type I test set up, the beam was loaded by a concentrated load at midspan (Fig. 6) and in Type II test specimens, the beam was loaded by two concentrated loads by means of a cross beam (Fig. 7) to provide a pure bending region in the central portion of the beam as shown in Fig. 8. The shear and bending diagrams for each type of test setup are shown in Figs. 8 and 9. The loads were applied at a shear distance, L, from the centerline of the closest support. Dial gauges and strain gages were mounted at the middle of the span to record the deflection of beam specimens and the strain of steel channel. Figures 10 and 11 show the load versus deflection for beam specimens S-1 and B-4 and Figures 12 and 13 are the graphical representation of stress-strain relationship for test specimens S-1 and B-4.

All beam specimens were tested to failure by using 300,000.00 lb Olson tension testing machine as shown in Figs. 6 and 7. Figures 14 and 15 show the typical failure patterns for bending and

shear test specimens, respectively. For each test specimen, the ultimate failure load, P_u, and other experimental data were recorded and listed in Table 2. The experimentally determined bending capacity, M_u, and shear strength capacity, V_u, computed on the basis of failure load, P_u, are given in Tables 3 and 4. Other experimental and analytical results are also presented in these two tables.

EVALUATION OF TEST RESULTS

The test results from the experienmental studies were carefully analyzed and evaluated to determine the bending and shear strength of the composite beams and the behavior of these members subjected to combined bending and shear.

Bending Strength

In general the composite cold-formed steel-concrete beams are unshored and the cold-formed steel soffits have to possess adequate strength and stiffness to support wet concrete loads. In this case, the maximum bending stress in the cold-formed steel channels can be computed by elastic theory using moment and deflection coefficients determined from structural analysis with span taken as distances between reaction points as expressed by the following formula:

$$f = \frac{M_{wc} \cdot y}{I_s} \quad \text{.....(1)}$$

in which M_{wc} is the bending moment due to wet concrete; y is the distance from the neutral axis to the outside fiber of the channel section; I_s is the moment of inertia of the channel section with respect to its neutral axis.

Once the concrete has been cured and hardened, the section acts as a composite reinforced concrete member and the ultimate strength concept in reinforced concrete design can be applied to determine the bending capacities of beam specimens [2,9]. In this case the composite beams can be classified as underreinforced or overreinforced depending on the amount of steel ratio, $\rho = A_s/bd$. The ratio of steel that produces a balance condition for a composite cold-formed steel-reinforced concrete beam can be computed by using the same formula for composite steel-deck slab as indicated in the following equation [4,7]:

$$\rho_b = \frac{0.85\,\beta_1 f'_c}{f_y} \cdot \frac{88{,}500(D-d_d)}{(88{,}500+f_y)d} \quad \text{.....(2)}$$

where $\beta_1 = 0.85$ for concrete with $f'_c \leq 4{,}000$ psi and reduced at a

rate of 0.05 for each 1,000 psi of strength exceeding 4,000 psi; however, β_1 shall not be less than 0.65; f_y = specified yield point or yield strength of steel, psi; D = overall depth of composite beam; d_d = overall depth of cold-formed steel soffit channel; d = effective depth of composite beam, in.

Beams which have a reinforcement ratio less than or equal to that which produces balanced conditions are considered to be underreinforced, whereas beams with a reinforcement ratio greater than that given by Equation 2 are considered overreinforced.

For underreinforced case, the ultimate moment, M_u, of beam specimens can be computed by the following formula:

$$M_u = A_s f_y (d - a/2) \quad \text{.....(3)}$$

in which A_s = cross-sectional area of soffit; f_y = yield point of steel; d = distance from extreme compression fiber to the centroid of soffit; and a = depth of the effective compressive zone of concrete as shown in Equation 4:

$$a = \frac{A_s f_y}{0.85 f'_c b} \quad \text{.....(4)}$$

If the beam specimen is underreinforced, the bending moment, M_u, can be determined by strain compatibility.

The computed ultimate moment capacities, $(M_u)_c$, for 4 bending beam specimens B-1 to B-4 were computed on the basis of Equation 3 and the results are tabulated in Table 3. The accuracy of Equation 3 in predicting the ultimate bending moment is indicated by the ratio of $(M_u)_c/M_u$ which is also listed in this table. The moment ratios range from 0.981 to 1.055 with a meam value of 1.023.

Shear Strength

The strength at which a flexure-shear crack forms is taken to be the shear strength of a beam without shear reinforcement and it can be computed by the following well known formula [2,9]:

$$V_{cr} = bd\left[1.9\sqrt{f'_c} + 2{,}500\,\rho\,\frac{Vd}{M}\right] \leq 3.5\,f'_c(bd) \quad \text{.....(5)}$$

in which $\rho = A_s/bd$; and V/M = the ratio of shear to bending moment occuring simulaneously.

The ability of a beam to carry additional load after an inclined crack has formed depends on whether or not the portion of shear formely carried by uncracked concrete can be redistributed across the inclined crack. In the case of cold-formed steel-concrete beams without shear reinforcement, it has been reported that the shear force is transmitted by the uncracked portion of concrete,

V_c, and across the steel channel as dowel action, V_d, [1]. The dowel force, V_d, creates vertical tension stresses at the location of the lips of the channel causing splitting of the concrete along the plane of the lips of the soffits.

The shear strength, V_{cr}, of 16 shear test specimens is computed on the basis of diagonal flexure-shear cracking as shown in Equation 5 and are tabulated in Table 3. This table also lists the ratio of V_{cr}/V_u between the flexure-shear crack and tested shear strength of all shear test specimens. This ratio ranges from 0.437 to 0.661 with an average value of 0.585 which indicates that the flexure-shear crack strength expressed in Equation 5 can not be used in predicting the ultimate shear capacities of composite cold-formed steel flexural members; however this equation can be used to determine a lower limit for the shear crack developments.

Shear-Bond Strength

In the past, several equations have been presented to compute the ultimate shear-bond capacity of composite steel deck slabs and the developing of these equations requires evaluation some unknown coefficients experimentally [1,5]. The number of experimental tests depends, in part on the desired level of accuracy of the computed ultimate shear-bond values. In 1970 Schuster [5,6] developed the following equation (Eq. 6) based on the hypothesis that failure is initiated by diagonal tension cracking, since

early experiments showed no end-slip prior to ultimate loads.

$$\frac{V_u}{\rho bd} = m\frac{d\sqrt{f'_c}}{\rho L} + k \qquad \text{.....(6)}$$

in which V_u, ultimate transverse shear-bond capacity; and m and k are constants obtained from experimental data.

It has been observed during the experimental investigation that before crack, the load is carried by both the steel channel and concrete. The embossments in the web of cold-formed steel channel soffits transmit shear forces between steel channel and concrete and both concrete and steel channel will deflect together. As the load increases, vertical separation is initiated at the location of maximum load, the composite action is no longer maintained and the concrete is essentially carrying additional load. This process will continue, more vertical separation, more load carried by concrete and more shear devices become disengaged. However in the case of cold-formed stiffened channels with the existence of the lips in the stiffened channels, the uplift of concrete and its separation from steel is reduced by the lips of the soffits in composite beams. The second stage of failure will be reached when the additional load carried by concrete becomes sufficently large to initiate a diagonal crack and finally the ultimate shear strength of the beam member is reached when the size of the cracks becomes excessively large and

the concrete shear-span becomes disengaged from the steel deck.

On the basis of the above discussion, it is suggested that the failure is initiated by vertical separation and embossment disengagement between concrete and cold-formed steel channel and the ultimate failure load is reached by a standard diagonal tension crack as in the case of reinforced concrete beam without shear reinforcement.

Based on the experimental data from 16 shear test specimens presented in Table 3, it was found that the ultimate shear strength, V_u, of composite cold-formed steel beams can be expressed by Equation 6 in which the values of the coefficients m and k are 9.0 and 1000.0, respectivelly by using regression analysis on the tested data (Fig. 16). Consequently, the shear-bond strength can be computed by the following equation:

$$\frac{V_u}{\rho bd} = 9.0 \frac{d\sqrt{f'_c}}{\rho L} + 1000.0 \quad \text{when } L/d < 4.5 \quad \ldots\ldots\ldots\ldots(7)$$

$$= 2.0 \frac{\sqrt{f'_c}}{\rho} + 1000.0 \quad \text{when } L/d \geq 4.5 \quad \ldots\ldots\ldots\ldots(8)$$

in which $\rho = A_s/bd$; f'_c = compressive strength of concrete; L = shear span; d = effective depth of composite beam; and b = width

of the beam.

By using Equations 7 and 8, the ultimate shear-bond capacities, $(V_u)_c$ of 16 beam specimens (S-1 to S-16), were computed and are listed in Table 3. The shear ratios of $(V_u)_c/V_u$ between computed and tested values are also tabulated in this table. These ratios varied from 0.901 to 1. 136 with an average value of 1.001 which indicate that good agreement was obtained between tested and computed shear-bond strength of these beam members.

The comparison of the tested and computed shear-bond strength is also represented graphically in Fig. 17, which indicates that Equations 7 and 8 adequately predict the shear strength of composite cold-formed steel composite beams within +15% and -15% of the tested value.

COMBINED BENDING AND SHEAR

Unlike composite steel-concrete slabs, the span lengths of composite cold-formed steel-concrete beams are usually longer and as a result these flexural members are subjectd to a combination of bending and shear stresses. Attempt has been made in this experimental investigation to study the bebavior of these members by careful evaluation of 12 test specimens (C-1 to C-12). The bending and shear capacities of these specimens were computed on the basis of Equations 3, 7 and 8 and are listed in Table 4. Also tabulated in this table are the ratios of $V_u/(V_u)_c$ and $M_u/(M_u)_c$

between the tested and computed values for shear and bending. The ratios of $V_u/(V_u)_c$ varied from 0.695 to 1.030 and the ratios of $M_u/(M_u)_c$ ranged from 0.691 1.073 which indicate that if the beam members are subjected to large bending and shear stresses, their capacities will be reduced. Figure 18 is a graphical representation of the relationship between the two ratios of $V_u/(V_u)_c$ and $M_u/(M_u)_c$ of the beam specimens which also shows a reduction in their capacities.

On the basis of test data given in Table 4, the conservative interaction formula as indicated in the the following formula has been developed as shown in Fig. 18:

$$\frac{V_u}{(V_u)_c} + \frac{M_u}{(M_u)_c} = 1.7 \quad \text{.....(9)}$$

Figure 18 shows the relationship of $V_u/(V_u)_c$ and $M_u/M_u)_c$ as obtained from presented test program. These results are limited and additional testing is required before conclusive evaluation of the validity of Equation 9 is reached for design purposes. However, the test results indicated that there is a reduction in the shear strength of the beam members when the momemt ratio is larger than 0.6.

SUMMARY

An experimental investigation was conducted to study the feasibility of using cold-formed steel channels as reinforcements for cast-in-place concrete beams. Based on the results of 32 full size beam specimens, it was found that composite cold-formed steel-concrete beams lead to considerable savings in the cost and time of construction without increasing the area of steel required for reinforcement. Empirical formulas were also developed for predicting the shear-bond strengths, the bending capacities and the shear-bending interaction of composite beam members.

ACKNOWLEDGMENTS

This investigation was partially supported by California State University Long Beach Foundation. Some material used in this experimental work was donated by Century Construction Co. and CSM Metal Fabricators, Inc. Special thanks are also extended to Andrew Wong and Anas Aswad for their assistance in conducting the tests.

APPENDIX I. - REFERENCES

1. Abdel-Sayed, G., "Composite Cold-Formed Steel Concrete Structural Systems," Proceedings of the Sixth International Specialty Conference on Cold-Formed Steel Structures, University of Missouri-Rolla, Rolla, Mo., November, 1982
2. "Building Code Requirements for Reinforced Concrete," ACI-318-83, American Concrete Institute, Detroit, Michigan, 1983.
3. Nguyen, R.P., and Yu, W.W., "Laterally Reinforced Cold-Forced Steel Beam Webs," Journal of the Structural Division, ASCE, Vol. 108, No. ST11, November, 1982.
4. Porter, M.L., and Ekberg, C.E., Jr., "Design Recommendations for Steel Deck Floor Slabs," Journal of the Structural Division, ASCE, Vol. 102, No. ST11, November, 1976.
5. Schuster, R.M.,"Composite Steel-Deck Concrete Floor Systems," Journal of the Structural Division, ASCE, Vol. 102, No. ST11, May, 1976.
6. Schuster, R.M., and Saleim, S.S., "Shear-Bond Capacity of Composite Slabs," Proceedings of the Sixth Specialty Conference on Cold-Formed Steel Structures, University of Missouri-Rolla, Rolla, Mo., November, 1982.
7. "Specification for the Design and Construction of Composite Slabs," American Society of Civil Engineers, New York, New York, October, 1984.
8. "Specification for the Design of Cold-Formed Structural Members," American Iron and Steel Institute, Washington, D.C., 1980.

9. Wang, C.K., and Salmon, C.G., Reinforced Concrete Design, Harper & Row, Publishers, New york, 1985.

10. Winter, G., "Cold-Formed Light Gage Steel Construction," Journal of the Structural Division, ASCE, Vol. 85, No. ST9, November, 1959.

11. Yu, W.W., Cold Formed Steel Design, John Wiley & Sons, Inc., 1985.

APPENDIX II. - NOTATION

The following symbols are used in this paper:

A_s = cross-sectional area of cold-formed steel channel or reinforcing bars;

a = effective depth of compression zone of concrete;

a1,a2 = width of stiffened lips of the channel;

b = width of composite beam;

b1 = depth of channel;

c = distance from extreme tension fiber to the centroid of the channel;

d = distance from extreme compression fiber to the centroid of the channel;

d_d = overall vertical depth of channel in composite beam;

f'_c = compressive strength of concrete;

f_y = yield point of steel channel;

h = overall depth of composite beam;

h1,h2 = depth of stiffened flanges of channel;

I_s = moment of inertia of the steel channel about its centroid;

k = constant used in shear-bond equation;

L = shear length;

M = bending moment;

M_u = ultimate tested bending moment;

$(M_u)_c$ = ultimate computed bending moment;

M_{wc} = applied bending due to fresh concrete;

m = constant used in shear bond equation;

P_c = experimental load at the initiation of first crack;

P_u = tested ultimate load;

r = corner radius;

V = shear force;

V_{cr} = computed ultimate concrete shear force;

V_u = tested ultimate shear force;

$(V_u)_c$ = computed ultimate shear force;

y = distance between channel centroid and its edges; and

ρ = A_s/bd

TABLE 1. Cold-Formed Steel Soffit Channel Properties

Beam Specimen No.	Cross-Section Dimensions, in inches								F_y, in Kips per sq. inch	A_s, in square inch
	Thick.	a1	a2	b1	h1	h2	r	c		
(1)	(2)	(3)	(4)	(5)	(6)	(7)	(8)	(9)	(10)	(11)
S-1	0.0529	0.525	0.510	3.938	1.473	1.460	0.0469	0.462	46.54	0.4005
S-2	0.0548	0.504	0.503	3.911	1.506	1.506	0.0469	0.475	46.54	0.4156
S-3	0.0530	0.484	0.502	3.977	1.484	1.479	0.0469	0.458	46.54	0.4033
S-4	0.0515	0.478	0.492	3.954	1.481	1.467	0.0469	0.456	46.54	0.3844
S-5	0.0501	0.506	0.505	3.970	1.492	1.510	0.0469	0.470	46.54	0.3830
S-6	0.0500	0.515	0.494	3.973	1.490	1.483	0.0469	0.465	46.54	0.3817
S-7	0.0549	0.501	0.504	3.975	1.470	1.467	0.0469	0.463	43.37	0.3768
S-8	0.0510	0.510	0.488	3.970	1.473	1.465	0.0469	0.456	43.37	0.3865
S-9	0.0651	0.601	0.608	4.922	2.020	2.033	0.0469	0.642	43.37	0.6373
S-10	0.0652	0.607	0.598	4.925	2.032	2.024	0.0469	0.641	43.37	0.6383
S-11	0.0519	0.495	0.502	3.957	1.477	1.480	0.0469	0.461	43.37	0.3934
S-12	0.0520	0.497	0.499	3.932	1.474	1.470	0.0469	0.459	43.37	0.3920
S-13	0.0765	0.713	0.717	6.031	2.490	2.494	0.0469	0.783	43.37	0.9175
S-14	0.0745	0.720	0.706	6.016	2.472	2.508	0.0469	0.782	43.37	0.8925
S-15	0.0665	0.629	0.611	4.962	1.996	1.997	0.0469	0.632	43.37	0.6512
S-16	0.0671	0.606	0.628	4.964	1.987	1.989	0.0469	0.627	43.37	0.6554
B-1	0.0491	0.484	0.507	3.961	1.487	1.473	0.0469	0.460	43.37	0.3729
B-2	0.0501	0.502	0.505	3.962	1.462	1.465	0.0469	0.456	43.37	0.3795
B-3	0.0525	0.487	0.515	3.974	1.467	1.473	0.0469	0.457	43.37	0.3979
B-4	0.0510	0.492	0.517	3.954	1.471	1.472	0.0469	0.460	43.37	0.3866
C-1	0.0641	0.633	0.583	4.986	2.003	2.005	0.0469	0.630	43.37	0.6293
C-2	0.0620	0.634	0.577	5.023	1.987	2.006	0.0469	0.624	43.37	0.6105
C-3	0.0501	0.514	0.493	3.970	1.491	1.480	0.0469	0.464	43.37	0.3821
C-4	0.0499	0.501	0.502	3.972	1.472	1.464	0.0469	0.457	43.37	0.3787
C-5	0.0782	0.683	0.680	6.018	2.494	2.489	0.0469	0.774	43.37	0.9310
C-6	0.0751	0.687	0.673	6.016	2.504	2.474	0.0469	0.773	43.37	0.8943
C-7	0.0642	0.623	0.587	4.965	1.979	2.021	0.0469	0.628	43.37	0.6280
C-8	0.0664	0.636	0.578	5.036	1.988	2.008	0.0469	0.624	43.37	0.6536
C-9	0.0792	0.697	0.698	6.023	2.482	2.461	0.0469	0.771	43.37	0.9423
C-10	0.0806	0.685	0.679	5.998	2.505	2.478	0.0469	0.775	43.37	0.9570
C-11	0.0682	0.622	0.571	5.014	1.981	1.992	0.0469	0.618	43.37	0.6663
C-12	0.0656	0.624	0.588	4.981	1.984	1.998	0.0469	0.624	43.37	0.6413

Note: 1 in. = 25.4 mm; 1 ksi = 6.895 MPa; 1 sq. in. = 6.45 cm^2.

TABLE 2. Experimental Data for Beam Test Specimens

Beam Specimen No. (1)	h in inch (2)	b in inch (3)	d in inch (4)	f'_c in lbs per sq. in (5)	100ρ (6)	Total Length in inch (7)	L in inch (8)	P_c in inch (9)	P_u in Kips (10)	Failure Mode (11)
S-1	6.188	3.938	5.726	2916	1.776	34.0	17.0	3.50	8.51	S
S-2	6.063	3.911	5.588	2916	1.902	34.0	17.0	3.75	8.52	S
S-3	6.291	4.058	5.761	2916	1.725	54.0	17.0	3.95	8.94	S
S-4	6.234	4.075	5.775	2916	1.682	54.0	17.0	3.98	8.98	S
S-5	6.031	3.897	5.561	5157	1.776	34.0	17.0	4.75	10.15	S
S-6	6.125	3.973	5.660	5157	1.697	34.0	17.0	4.85	10.25	S
S-7	8.105	3.975	7.644	2916	1.374	36.0	18.0	7.80	13.40	S
S-8	8.125	3.970	7.669	2916	1.269	36.0	18.0	8.05	11.98	S
S-9	8.031	4.922	7.389	2916	1.752	36.0	18.0	9.50	16.40	S
S-10	7.969	4.925	7.328	2916	1.769	36.0	18.0	9.10	15.50	S
S-11	7.875	3.957	7.414	2916	1.341	36.0	18.0	9.15	13.28	S
S-12	7.938	3.932	7.479	2916	1.333	30.0	15.0	10.75	16.05	S
S-13	10.025	6.125	9.242	2916	1.621	45.0	22.5	15.25	21.50	S
S-14	9.875	6.105	9.093	2916	1.608	45.0	22.5	15.50	21.45	S
S-15	6.031	5.031	5.399	2916	2.397	44.0	12.0	6.50	12.80	S
S-16	6.125	5.188	5.498	2916	2.298	44.0	12.0	6.80	12.04	S
B-1	5.969	4.108	5.509	2916	1.648	81.0	30.0	-	5.18	B
B-2	5.938	3.959	5.482	2916	1.749	81.0	30.0	-	5.04	B
B-3	7.938	4.887	7.481	2916	1.088	81.0	32.0	-	6.92	B
B-4	8.031	4.814	7.571	2916	1.061	81.0	32.0	-	6.88	B
C-1	5.969	4.906	5.339	2916	2.403	81.0	40.5	-	6.10	C
C-2	6.016	4.938	5.392	2916	2.293	81.0	40.5	-	6.02	C
C-3	6.040	3.872	5.576	5157	1.770	36.0	18.0	-	9.70	C
C-4	6.128	3.971	5.671	5157	1.682	36.0	18.0	-	9.84	C
C-5	6.125	6.063	5.351	5157	2.870	44.0	21.0	-	12.25	C
C-6	6.063	6.125	5.290	5157	2.760	44.0	21.0	-	12.05	C
C-7	8.016	5.008	7.388	2916	1.697	81.0	40.5	-	6.42	C
C-8	7.984	5.063	7.360	2916	1.754	81.0	40.5	-	6.48	C
C-9	5.938	6.125	5.167	2916	2.977	81.0	40.5	-	7.40	C
C-10	5.969	5.984	5.194	2916	3.079	81.0	40.5	-	7.60	C
C-11	7.781	4.969	7.163	2916	1.872	44.0	22.0	-	10.95	C
C-12	7.750	5.125	7.126	2916	1.756	44.0	22.0	-	10.54	C

Note: 1 in. = 25.4 mm; 1 psi = 0.006895 MPa; 1 kip = 4.45 kN.

TABLE 3. Comparison of Experimental and Theoretical Data for Beam Test Specimens

Beam Specimen No.	Experimental Loads				Computed Loads						
	V_u in Kips	M_u in inch-Kips	$\frac{V_u}{\rho bd}$	$\frac{d\sqrt{f'_c}}{\rho L}$	V_{cr} in Kips	$(V_u)_c$ in Kips	$(M_u)_c$ in inch-Kips	$\frac{P_c}{P_u}$	$\frac{V_{cr}}{V_u}$	$\frac{(V_u)_c}{V_u}$	$\frac{(M_u)_c}{M_u}$
(1)	(2)	(3)	(4)	(5)	(6)	(7)	(8)	(9)	(10)	(11)	(12)
S-1	4.26	72.42	10.638	1022.97	2.65	4.09	90.14	0.411	0.622	0.960	1.245
S-2	4.26	72.42	10.248	933.24	2.58	3.91	90.10	0.440	0.606	0.917	1.244
S-3	4.47	80.46	11.084	1060.85	2.71	4.26	85.56	0.442	0.609	0.952	1.063
S-4	4.49	80.82	11.337	1090.61	2.73	4.17	83.28	0.443	0.609	0.926	1.030
S-5	5.08	86.36	13.156	1322.69	3.26	4.94	90.42	0.468	0.642	0.973	1.047
S-6	5.13	87.24	13.443	1408.91	3.39	5.22	92.10	0.473	0.661	1.018	1.056
S-7	6.70	120.60	16.055	1668.34	3.50	6.03	121.74	0.582	0.522	0.901	1.010
S-8	5.99	107.82	15.504	1813.00	3.54	6.69	114.27	0.672	0.590	1.117	1.060
S-9	8.20	147.60	12.869	1265.24	4.39	7.89	172.92	0.579	0.535	0.963	1.172
S-10	7.75	139.50	12.139	1242.74	4.35	7.78	171.47	0.587	0.562	1.003	1.229
S-11	6.64	119.52	16.802	1658.61	3.42	6.27	119.82	0.673	0.501	0.944	1.003
S-12	8.03	120.45	20.485	2019.84	3.51	7.52	120.52	0.670	0.437	0.936	1.001
S-13	10.75	193.50	11.715	1368.34	6.99	12.22	315.61	0.709	0.650	1.136	1.631
S-14	10.73	193.14	12.020	1357.16	6.82	11.79	302.46	0.723	0.638	1.099	1.566
S-15	6.40	76.80	9.830	1013.58	3.52	6.59	120.50	0.508	0.550	1.030	1.569
S-16	6.22	74.64	9.490	1076.63	3.68	7.01	124.86	0.565	0.592	1.127	1.728
B-1	2.59	77.70	6.946	601.71	2.49	2.82	76.25		0.961	1.089	0.981
B-2	2.52	75.60	6.640	564.19	2.40	2.72	76.43		0.952	1.081	1.011
B-3	3.46	110.72	8.696	1160.31	3.98	4.55	116.81		1.150	1.316	1.055
B-4	3.44	110.08	8.898	1204.15	4.58	4.58	115.16		1.154	1.330	1.046

Note: 1 kip = 4.45 kN; 1 in.-kip = 113 N-m..

TABLE 4. Comparison of Experimental and Theoretical Data for Beam Test Specimens

Beam Specimen No.	Experimental loads			Computed Loads			$\frac{V_{cr}}{(V_u)_c}$	$\frac{V_u}{(V_u)_c}$	$\frac{M_u}{(M_u)_c}$
	P_u in Kips	V_u in Kips	M_u in inch-Kips	V_{cr} in Kips	$(V_u)_c$ in Kips	$(M_u)_c$ in inch-Kips			
(1)	(2)	(3)	(4)	(5)	(6)	(7)	(8)	(9)	(10)
C-1	6.10	3.05	123.53	2.89	3.46	115.09	0.835	0.882	1.073
C-2	6.02	3.01	121.91	2.93	3.49	114.13	0.840	0.862	1.068
C-3	9.70	4.85	87.30	3.24	4.71	78.10	0.688	1.030	1.035
C-4	9.84	4.92	88.56	3.37	4.96	85.39	0.679	0.992	1.037
C-5	12.25	6.13	128.73	5.02	6.27	185.37	0.810	0.963	0.694
C-6	12.05	6.03	126.63	4.98	6.17	177.16	0.807	0.997	0.715
C-7	6.42	3.21	130.00	4.08	4.62	171.34	0.883	0.695	0.759
C-8	6.84	3.42	138.51	4.12	4.68	176.62	0.880	0.731	0.784
C-9	7.40	3.70	149.85	3.55	4.36	156.16	0.814	0.849	0.960
C-10	7.60	3.80	153.90	3.50	4.31	157.51	0.812	0.882	0.977
C-11	10.95	5.48	120.56	4.19	6.30	173.09	0.665	0.870	0.697
C-12	10.54	5.27	115.94	4.27	6.40	167.75	0.667	0.823	0.691

Note: 1 kip = 4.45 kN; 1 in.-kip = 113 N-m.

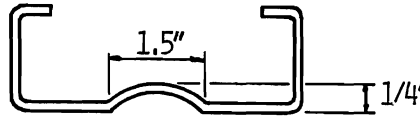

SECTION

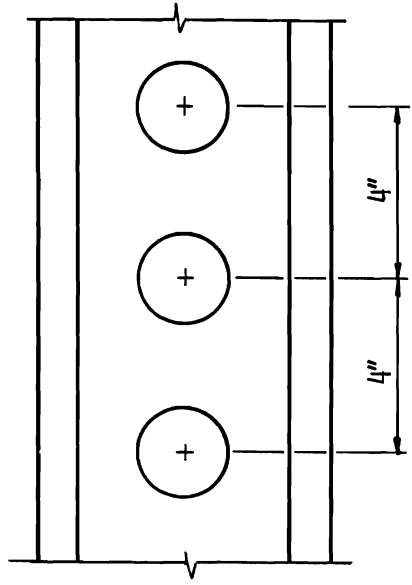

FIG. 1. - COLD-FORMED STEEL CHANNEL WITH EMBOSSEMENT

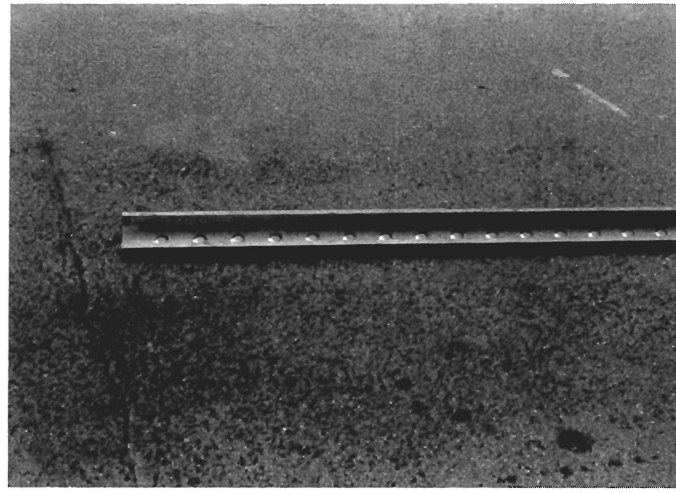

FIG. 2. - COLD-FORMED STEEL CHANNEL

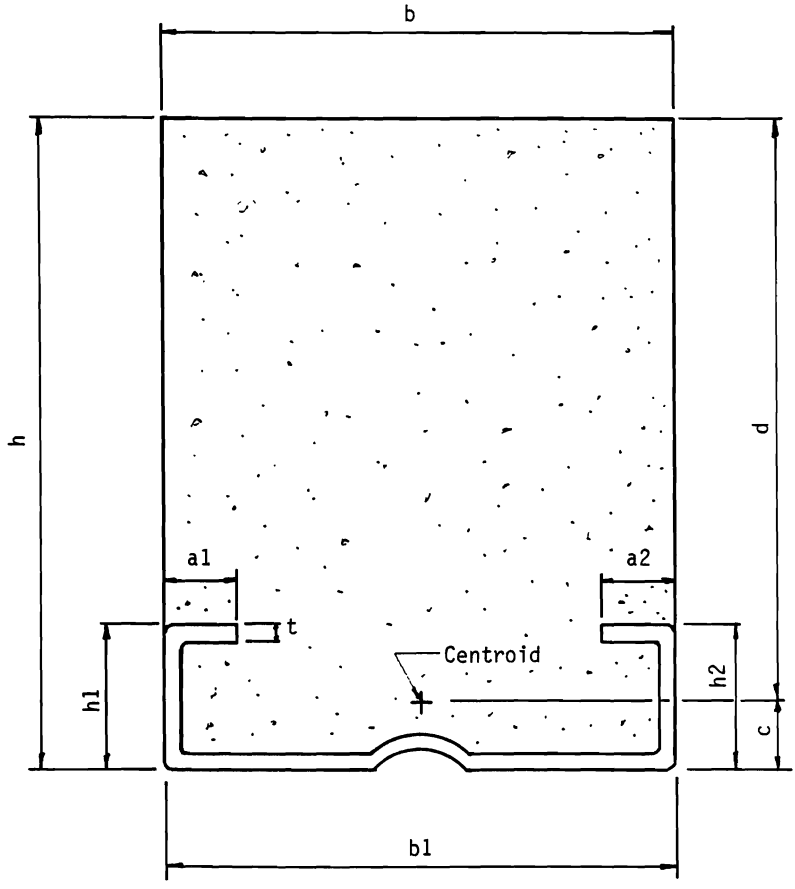

FIG. 3. - TYPICAL COMPOSITE BEAM SECTIONS

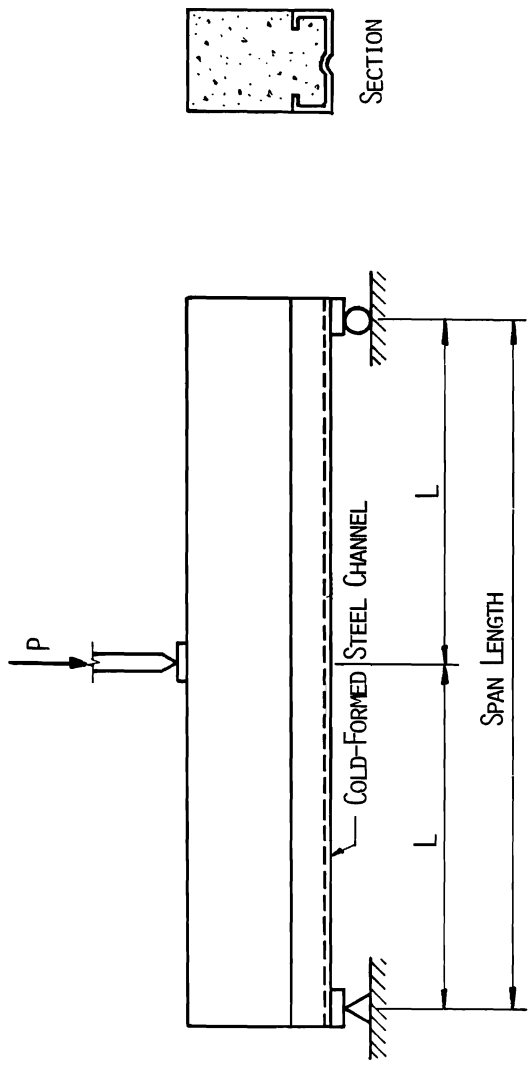

FIG. 4. - TEST SETUP TYPE I

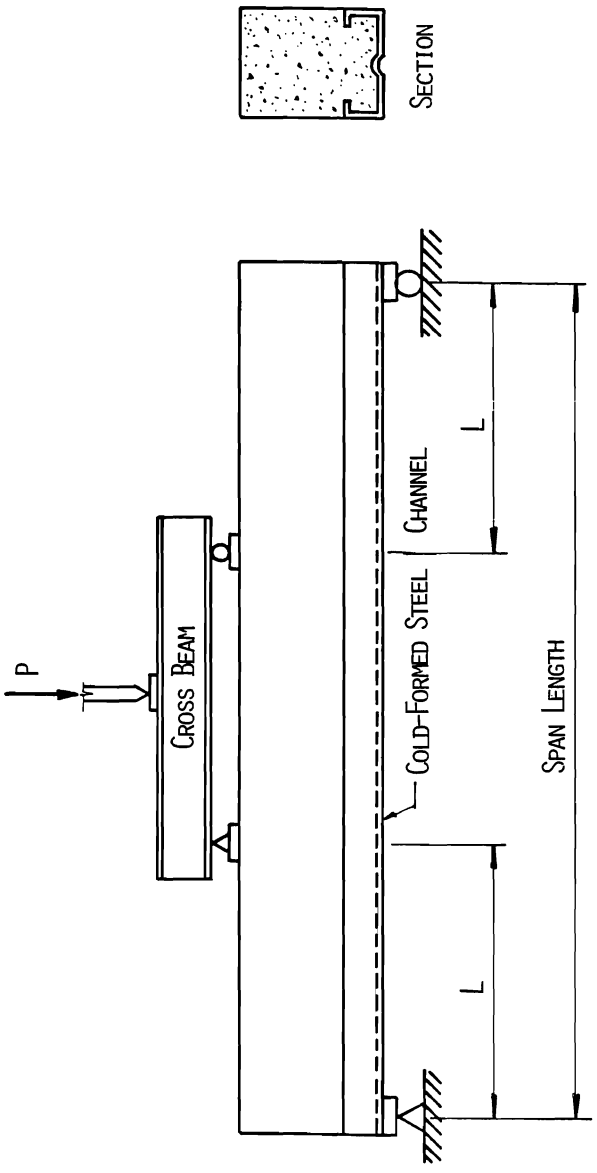

FIG. 5. - TEST SETUP TYPE II

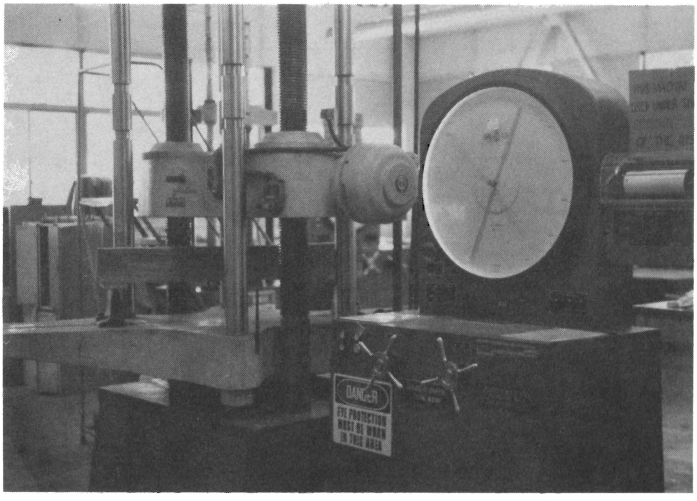

FIG. 6. - Test Setup Type I

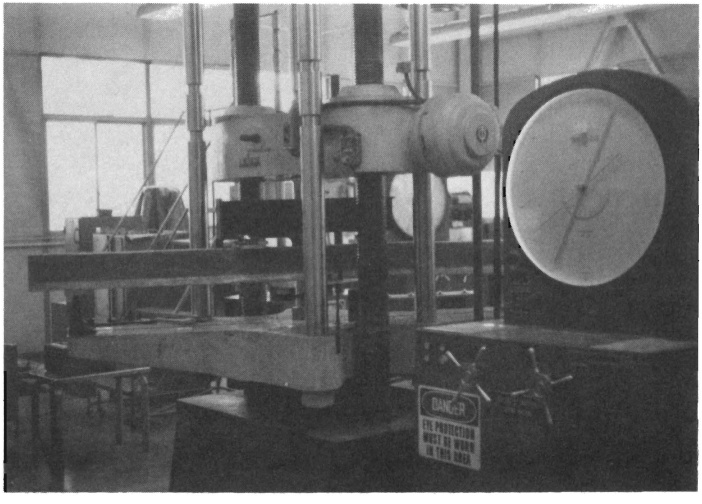

FIG. 7. - Test Setup Type II

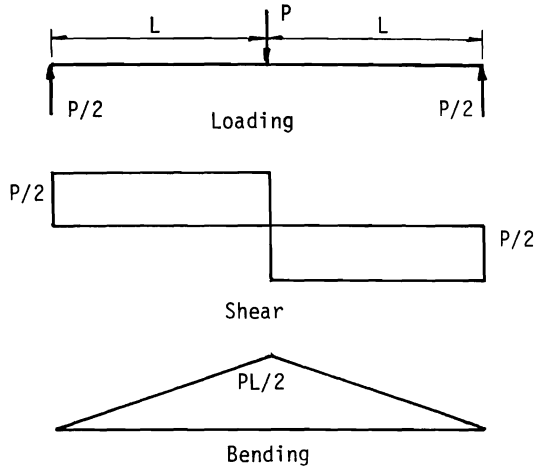

FIG. 8. - Shear and Bending Diagrams

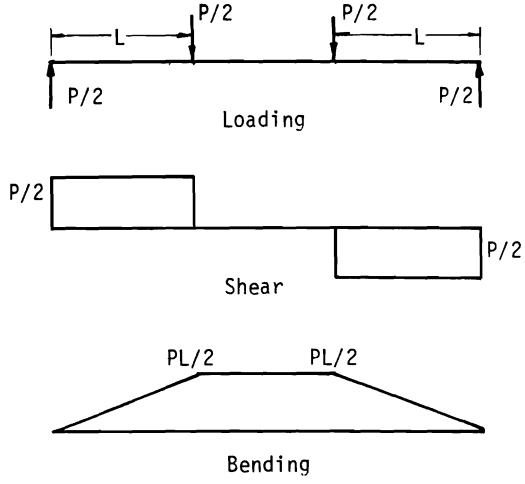

FIG. 9. - Shear and Bending Diagrams

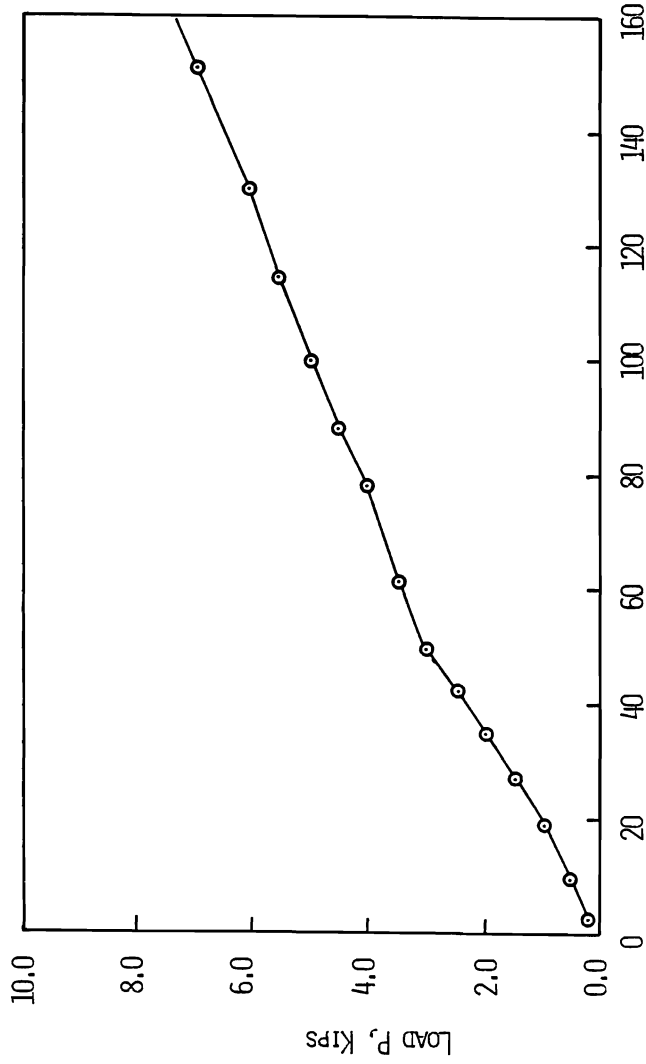

FIG. 10. - LOAD VERSUS DEFLECTION FOR BEAM SPECIMEN S-1

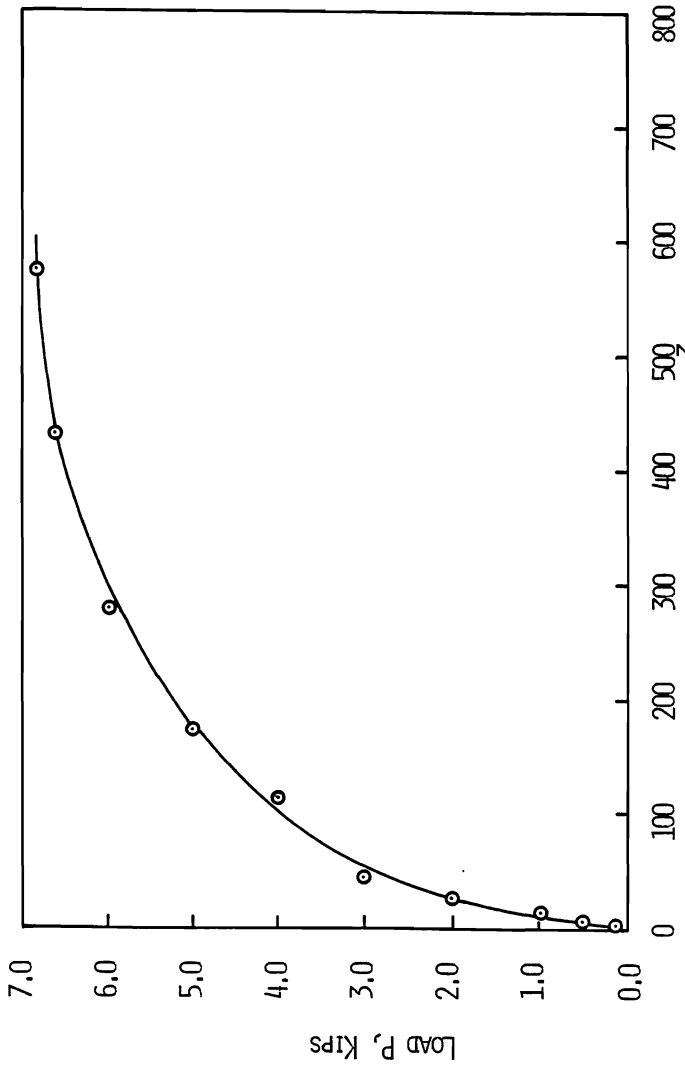

FIG. 11. - Load P versus Deflection for Beam Specimen B-4

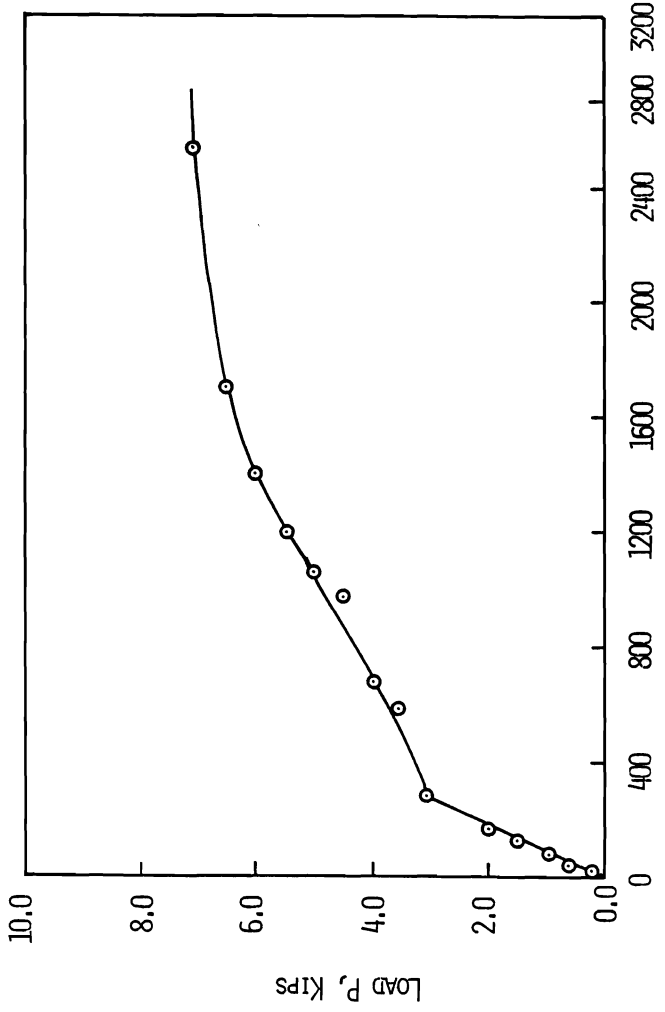

FIG. 12. - LOAD P VERSUS STRAIN FOR BEAM SPECIMEN S-1

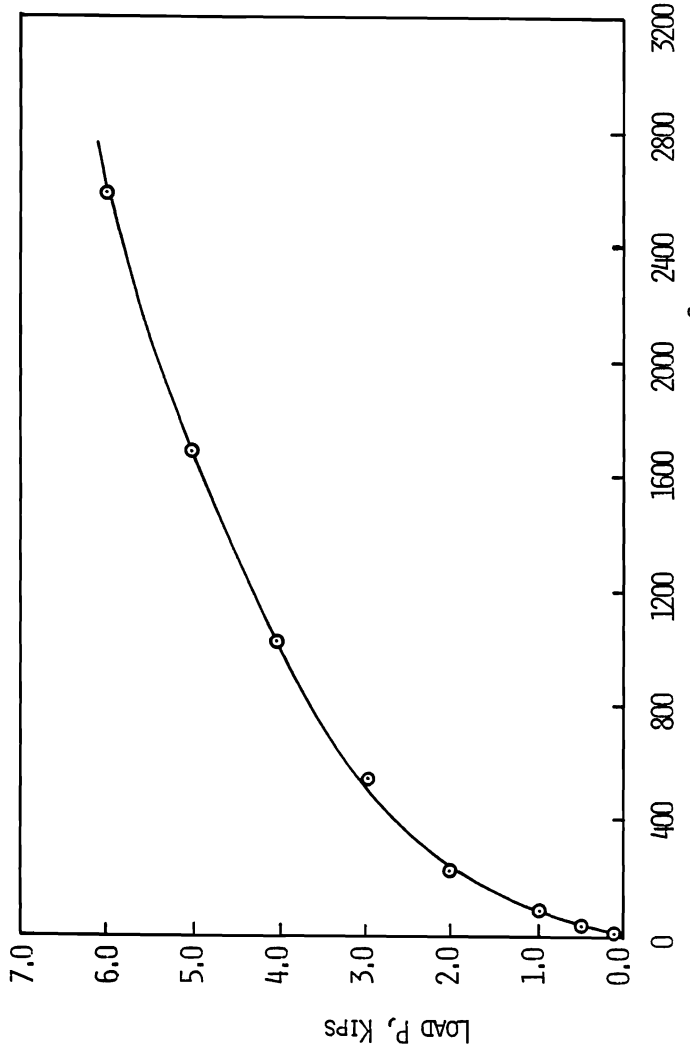

FIG. 13, - Load versus Strain for Beam Specimen B-4

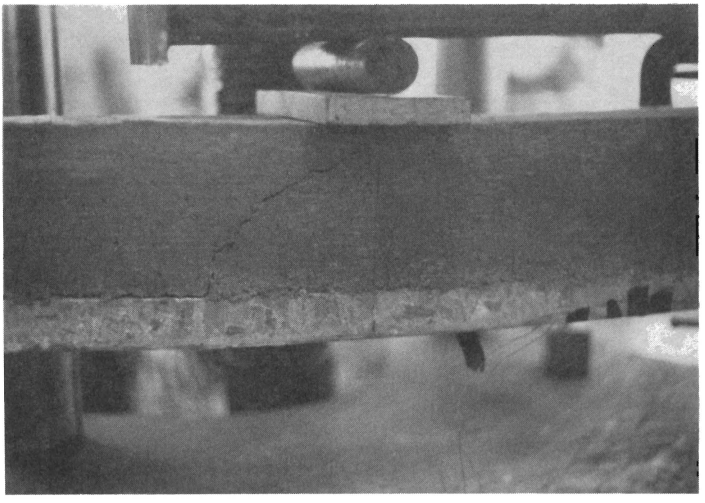

FIG. 14. - TYPICAL FAILURE PATTERN FOR SHEAR TEST SPECIMENS

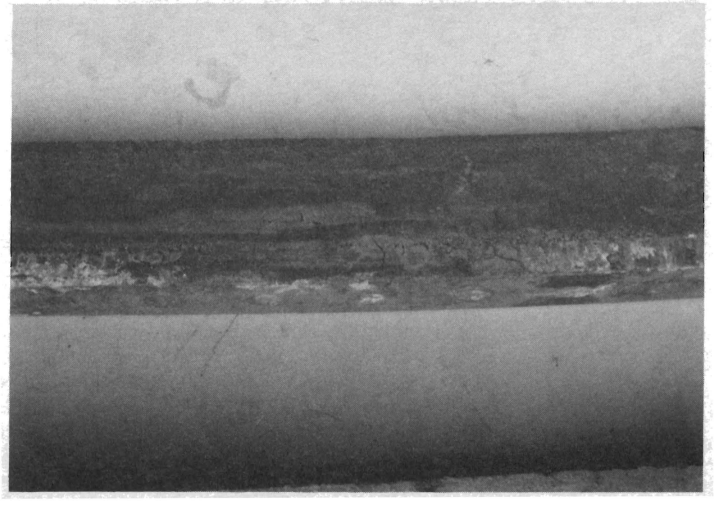

FIG. 15. - TYPICAL FAILURE PATTERN FOR BENDING TEST SPECIMENS

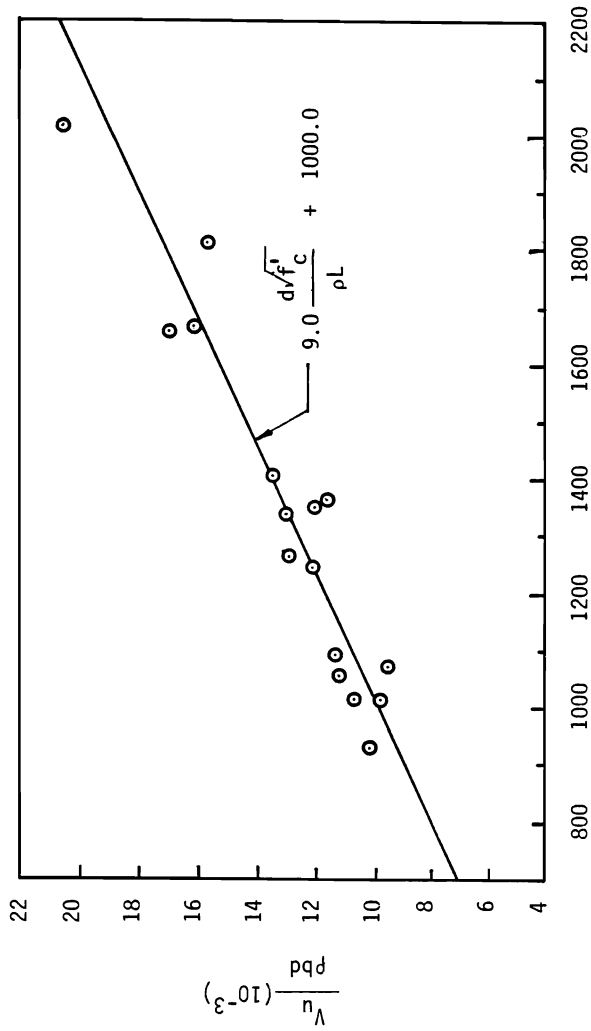

FIG. 16. - RELATIONSHIP BETWEEN $V_u/\rho bd$ AND $d\sqrt{f'_c}/\rho L$

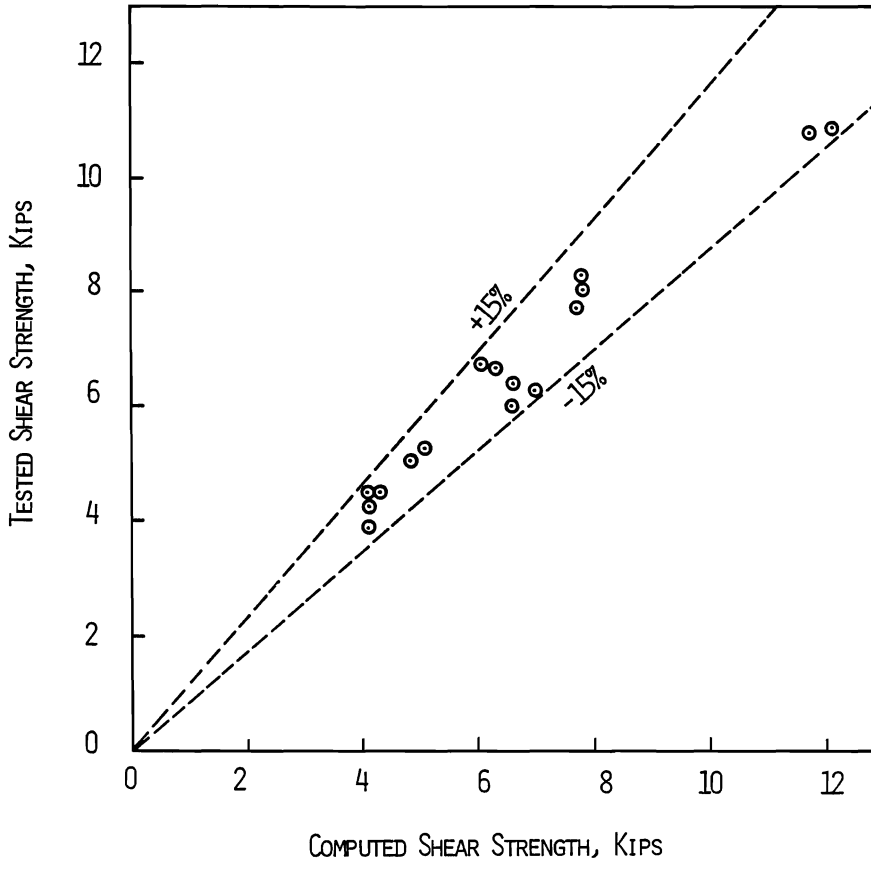

FIG. 17. - CORRELATION BETWEEN TESTED AND COMPUTED SHEAR STRENGTH

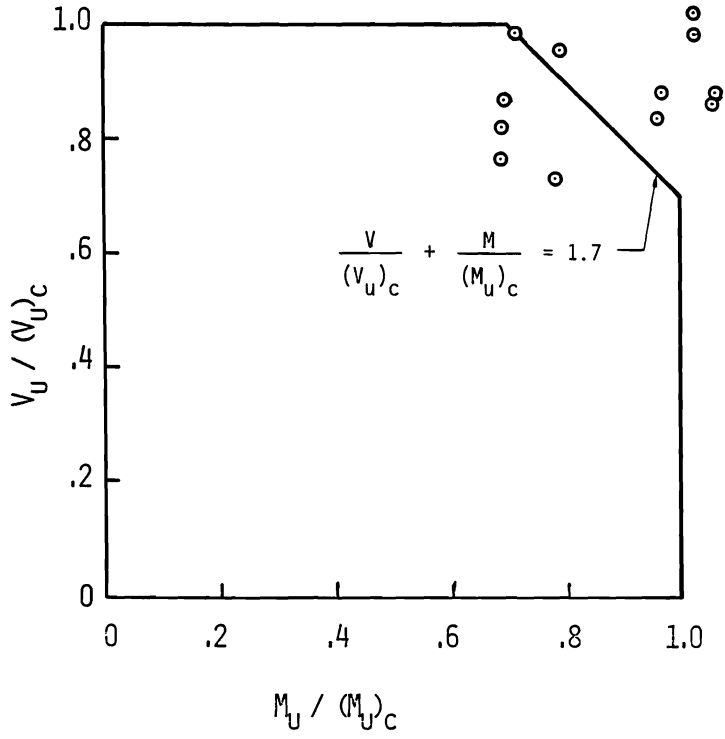

FIG. 18. - RELATIONSHIP BETWEEN $V_U / (V_U)_C$ AND $M_U / (M_U)_C$